Microwave Reflectance Studies of Photoelectrochemical Kinetics at Semiconductor Electrodes. 3. Photolectrochemical Reduction of $Ru(NH_3)_6^{3+}$ at p-Si

Laurence M. Peter* and Shin Ushiroda[†]

Department of Chemistry, University of Bath, Bath BA2 7AY, United Kingdom

Received: October 28, 2003; In Final Form: December 16, 2003

The reduction of $Ru(NH_3)_6^{3+}$ at illuminated p-Si in ammonium fluoride solutions was studied by a light modulated microwave reflectivity method. $Ru(NH_3)_6^{3+}$ was chosen as an example of a one electron outer sphere redox system that is expected to exhibit facile electron transfer kinetics. The results of the microwave measurements show that the transfer of photogenerated electrons to $Ru(NH_3)_6^{3+}$ at an illuminated p-Si electrode is very slow compared to an order of magnitude estimate for outer sphere electron transfer. It is concluded that the reduction of $Ru(NH_3)_6^{3+}$ does not involve direct electron transfer from the conduction band but is instead mediated by photogenerated hydrogen states.

Introduction

Investigation of the kinetics of electron transfer at illuminated semiconductor electrodes is complicated by the fact that only limited information is available from the measured photocurrent. In the case of a semiconductor electrode biased into strong depletion, photogenerated carriers are swept to the interface by the electric field in the space charge region, and the measured current is simply proportional to the light intensity. Transient photocurrent measurements in the photocurrent saturation region at high band bending also contain no information about the rate constants for electron transfer because it is not possible to distinguish between the displacement current and the transfer of electrons across the interface. Information about the kinetics of interfacial electron transfer can be obtained by studying the transient or periodic photocurrent response in the photocurrent onset region at lower bias, where recombination competes with electron transfer. An example of a technique that exploits this competition is intensity modulated photocurrent spectroscopy (IMPS), which involves measuring the frequency-dependent magnitude and phase of the photocurrent response to a sinuosoidally modulated photon flux.[1,2] More recently, we have developed an analogous modulation technique that involves measuring the periodic change in microwave reflectivity caused by intensity modulated illumination.[3−5] The use of microwave reflectivity measurements for the characterization of semiconductor electrodes was pioneered by Tributsch and co-workers.[6−8] The method is sensitive to changes in the conductivity of a semiconductor sample brought about by illumination or changes in applied voltage. In the case of photoelectrochemical reactions, minority carriers are driven to the surface, where they may accumulate in substantial concentrations if electron transfer to redox species is a slow process. The buildup and decay of these charge carriers when the illumination is switched on and off is determined by the rate of interfacial charge transfer. The accumulation of photogenerated carriers near the interface is not evident in the current transient, but it can be followed by the change in conductivity detected by microwave reflectance.[9] This is the basis of the light modulated microwave reflectivity (LMMR) technique.[3−5] The present paper describes the application of LMMR to study the photoreduction of ruthenium(III) hexaammine at illuminated p-Si under conditions where the silicon surface is free of oxide. This system was chosen to test the expectation that rapid capture of photogenerated electrons by $Ru(NH_3)_6^{3+}$ should prevent the buildup of electrons and hence effectively quench the microwave response completely, as predicted by our recent theoretical modeling.[4] In fact, the study revealed that the microwave response is not quenched by the presence of $Ru(NH_3)_6^{3+}$. Consequently, it proved possible to measure the rate constant for electron transfer, which turns out to be many orders of magnitude smaller than expected. The reasons for this surprising result are explored.

Theory

Definition and Estimation of Rate Constants. Discussion of electron transfer at semiconductor electrodes is complicated by the fact that three different rate constants are commonly used. The rate of electron transfer is first order in the concentration of electrons or holes in the semiconductor and also first order in the concentration of redox species in the electrolyte. The starting point for the discussion is therefore the second-order heterogeneous rate constant for interfacial electron transfer, k_2 ($cm^4\ s^{-1}$). If the concentration of redox species in the interfacial region is assumed to be constant, a pseudo-first-order heterogeneous rate constant for electron transfer, k_{tr} ($cm\ s^{-1}$), can be defined that is analogous to the rate constant used to describe electron transfer at a metal contact. Finally, a phenomenological electron transfer rate constant, k_1 (s^{-1}), can be defined[10] by introducing the concept of an effective *surface* electron or hole density (cm^{-2}). The relationship between the three rate constants can be expressed in the form

$$k_1 = \frac{k_{tr}}{\delta} = \frac{k_2 N_{redox}}{\delta} = \upsilon_{th}\sigma_{redox}N_{redox} \qquad (1)$$

Here δ is a nominal reaction layer thickness or tunneling length for electron transfer at the interface, υ_{th} is the thermal velocity of minority carriers, and σ_{redox} is the capture cross section for the reaction of minority carriers with redox species present with a volume density of N_{redox} in the solution.[11]

[†] Current address: Department of Chemistry, Colorado State University, Fort Collins, Colorado 80523.

10.1021/jp0311963 CCC: $27.50
Published on Web 01/27/2004

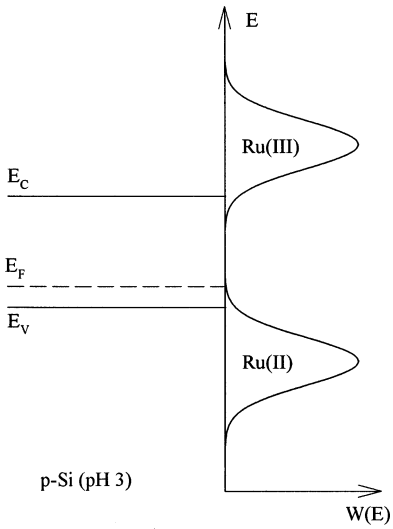

Figure 1. Energy scheme for capture of photogenerated electrons from the conduction band of low-doped p-Si in ammonium fluoride electrolyte (pH 3.0). Note that the overlap between conduction band states and Ru(III) states is expected to facilitate rapid electron transfer.

The Ru(III)/Ru(II) hexaammine redox system is relatively substitution inert, and the homogeneous self-electron self-exchange rate constant of the couple at 298 K is reported[12] to be 2.2×10^4 M^{-1} s^{-1}, which is consistent with values of the standard heterogeneous rate constant of the order of 1 cm s^{-1} at metal electrodes. These rate constants correspond to a value of about 0.9 eV for the reorganization energy for outer sphere electron transfer from a semiconductor electrode. The standard potential of the couple places the redox Fermi level close to the center of the band gap of silicon in fluoride solutions at pH 3, so that rapid transfer of photogenerated electrons from the conduction band of p-Si to Ru(III) should be possible, as illustrated by Figure 1.

The electron transfer rate constant k_2 can be expressed in the form[13]

$$k_2 = \upsilon \kappa_n \kappa_{el} \tag{2}$$

where κ_n is the (dimensionless) nuclear term related to the Franck Condon factor for the process, and κ_{el} (units cm^4) is determined by the electronic coupling between the reactants. The nuclear term is given by the well-known expression

$$\kappa_n = \exp\left[-\frac{(\Delta G^{0\prime} + \lambda)^2}{4\lambda k_B T}\right] \tag{3}$$

where $\Delta G^{0\prime}$ is the driving force for interfacial electron transfer and λ is the reorganization energy. On the basis of this approach, Royea et al.[14,15] have estimated an upper limit for the second-order rate constant k_2 for outer sphere reactions at semiconductor electrodes in the range $(1-10) \times 10^{-17}$ cm^4 s^{-1}. In the present case, using $\Delta G^{0\prime} = -0.5$ eV (cf. Figure 1) and $\lambda = 0.9$ eV for the ruthenium hexaammine couple gives an estimate of 0.18 for κ_n. On the basis of measurements of charge transfer at n-InP[13] and n-Si,[16] Lewis and co-workers have estimated κ_{el} to be of the order of 10^{-30} cm^4 s^{-1}, so that setting $\upsilon = 10^{13}$ s^{-1} gives $k_2 \approx 2 \times 10^{-18}$ cm^4 s^{-1} for electron transfer from the conduction band of p-Si to $Ru(NH_3)_6^{3+}$ at pH 3. For $[Ru(NH_3)_6^{3+}] = 10^{-2}$ M and $\delta = 10^{-7}$ cm, this value of k_2 corresponds to $k_{tr} = 12$ cm s^{-1} and $k_1 = 1.2 \times 10^8$ s^{-1}. As the next section shows, this order of magnitude estimate of the electron transfer rate constants predicts that the microwave response should be very small in the presence of $Ru(NH_3)_6^{3+}$, and the time constant for the transient and periodic responses should be correspondingly short (on the submicrosecond scale). The present study has shown that neither of these predictions is correct.

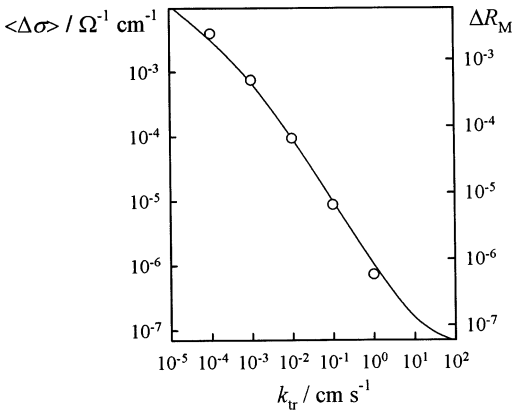

Figure 2. Solid line: dependence of the change in mean conductivity $\langle\Delta\sigma\rangle$ on the rate constant for interfacial charge transfer, calculated from the excess carrier profiles in the photocurrent saturation region (see ref 4 for details). Open circles: values of the microwave reflectance change ΔR_M calculated using a multilayer model and the Fresnel equations. Comparison of the two plots allows calculation of the sensitivity factor, *S*. Incident photon flux (626 nm) 10^{14} cm^{-2} s^{-1}. Note that the microwave response will be difficult to measure at this light intensity if $k_{tr} > 1$ cm s^{-1}.

Origin and Magnitude of the Microwave Response. The theoretical basis for microwave reflectivity measurements and LMMR has been reviewed recently, and the results of numerical calculations of the microwave reflectivity response for low-doped silicon of the type used in the present experiments have been presented.[4] Only the main points will be summarized here. The microwave reflectivity change ΔR_M brought about by perturbation of a semiconductor electrode by light can be related linearly to the change in mean conductivity, $\langle\Delta\sigma\rangle$, by

$$\Delta R_M = \frac{\Delta P_r}{P_i} = R_M \frac{\Delta P_r}{P_r} = S\langle\Delta\sigma\rangle = \frac{Sq}{d}\int_0^d [\mu_n \Delta n(x) + \mu_p \Delta p(x)]\, dx \tag{4}$$

Here P_i and P_r are the incident and reflected microwave power, respectively, ΔP_r is the change in reflected microwave power, R_M is the unperturbed microwave reflectivity, *S* is a sensitivity factor, *d* is the sample thickness, *q* is the elementary charge, $\Delta n(x)$ and $\Delta p(x)$ are the position dependent excess electron and hole densities resulting from illumination, and μ_n and μ_p are the electron and hole mobilities. The density profiles of photogenerated electrons and holes can be calculated for given conditions (intensity and wavelength of illumination and rate constant for interfacial electron transfer). Integration of the profiles then gives the change in mean conductivity and hence the microwave response. *S* can be measured[5] or it can be calculated using a filter stack model to represent the carrier profiles.[4]

Figure 2 indicates how the magnitude of the microwave reflectivity response for the experimental conditions used in this study is expected to decrease as the rate constant for electron transfer increases (further details are given in ref 4). Because the practical detection limit lies around $\Delta R_M = 10^{-6}$, it is clear that the microwave response should become undetectable once the rate constant k_{tr} exceeds $1-10$ cm s^{-1}.

Periodic Microwave and Photocurrent Response to Intensity Modulated Illumination. The time constant for the

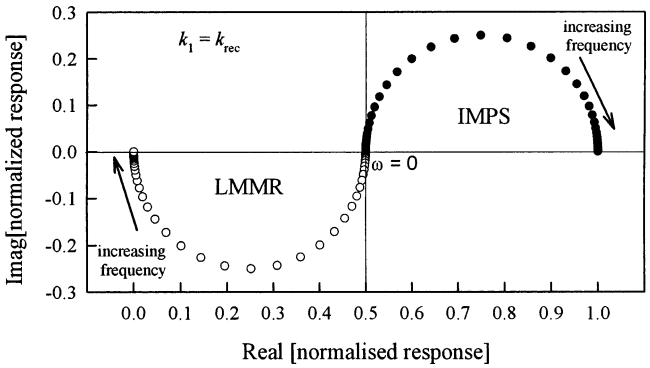

Figure 3. Comparison of LMMR and IMPS responses for the case where half of the photogenerated electrons are lost by surface recombination, i.e., $k_1 = k_{rec}$. It is important to note that the diameter of the LMMR semicircles increases as the band bending increases, whereas the IMPS semicircles become progressively smaller until all information is lost when the photocurrent saturation condition ($k_{rec} \ll k_1$) is reached.

microwave response to step and sinusoidal illumination profiles is given by[4]

$$\tau = (k_1 + k_{rec})^{-1} \quad (5)$$

where k_1 and k_{rec} are first-order rate constants (s^{-1}) for electron transfer and electron−hole recombination, respectively, that arise from a phenomenological formulation of kinetics in terms of the nominal surface concentrations (cm^{-2}) of electrons and holes.[10] As we have shown elsewhere,[3−5] values of k_1 and k_{rec} can be obtained by analysis of the light modulated microwave reflectivity (LMMR) response. The real and imaginary components of the normalized LMMR response are given by

$$\frac{1}{S}\mathrm{Re}(\Delta R_M) = \frac{k_1(k_1 + k_{rec})}{(k_1 + k_{rec})^2 + \omega^2}$$

$$\frac{1}{S}\mathrm{Im}(\Delta R_M) = -\frac{k_1\omega}{(k_1 + k_{rec})^2 + \omega^2} \quad (6)$$

where $\omega = 2\pi f$. The LMMR response is a semicircular plot in the complex plane with a low-frequency intercept determined by the ratio $k_1/(k_1 + k_{rec})$, a high-frequency intercept of zero and a minimum located at $\omega_{min} = 1/(k_1 + k_{rec})$. It is worth noting that in the absence of recombination ($k_{rec} \rightarrow 0$), the normalized plot has a low-frequency intercept of unity. By contrast, the corresponding normalized IMPS response is described by the expressions[1,2]

$$\mathrm{Re}\frac{j_{photo}}{qI_0} = \frac{\omega^2 + k_1(k_1 + k_{rec})}{(k_1 + k_{rec})^2 + \omega^2}$$

$$\mathrm{Im}\frac{j_{photo}}{qI_0} = \frac{\omega k_{rec}}{(k_1 + k_{rec})^2 + \omega^2} \quad (7)$$

Here I_0 is the absorbed photon flux. (For simplicity, it is assumed that all photoexcited minority carriers are collected in the space charge region.) The complex plane IMPS plots are characterized by a low-frequency intercept determined by the ratio $k_1/(k_1 + k_{rec})$ and a high-frequency intercept of unity. The difference between the IMPS and LMMR responses is illustrated in Figure 3 for the particular case where $k_1 = k_{rec}$; i.e., the dc photocurrent is half of the saturation value.

Experimental Section

Measurements were performed with a Ka-band microwave system and an experimental setup that have been described in detail elsewhere.[5] Boron doped p-Si (111) samples (ITME, 10−20 Ω cm doping density 7×10^{14} cm^{-3}) were used in the measurements. Samples were etched for 30 s in flowing CP-4A solution (3:5:3 by volume 48% HF: concentrated HNO_3: 100% CH_3COOH) and rinsed with Milli-Q water. Ohmic contact was made around the periphery of the wafer using Ga|In eutectic. The 1 M fluoride (pH 3) background electrolyte solution consisted of 0.5 M NH_4F (40%, BDH, Aristar), 0.15 M NH_4Cl (Aldrich, ACS reagent), and 0.5 M HF (48%, BDH, AnalaR). Hexaammine ruthenium(III) chloride (98%, Aldrich) was used to prepare the solutions with Ru(III) concentrations in the range 0.1−1.0 mM. The flow cell was designed to continuously refresh the solution layer above the illuminated p-Si electrode.The degassed electrolyte was circulated continuously through the PTFE flow cell via a gravity-fed reservoir by a nitrogen lift pump.

Measurements were made in three-electrode PTFE flow cell equipped with Pt wire counter and Ag/AgCl reference electrodes. Intensity-modulated photocurrent spectroscopy (IMPS) and light-modulated microwave reflectance (LMMR) measurements were performed by illuminating the sample with a red light emitting diode (LED: $\lambda = 626$ nm). Sinusoidal intensity modulation of the LED output was achieved by using a current driver programmed by the lock-in amplifier. The current and microwave responses were detected simultaneously by two synchronized lock-in amplifiers (Stanford Research SR830). A Stanford Research SR560 low-noise preamplifier was used to amplify the signal from the microwave detector. The illumination intensity was controlled using a set of calibrated Schott neutral density (NG) filters. Light intensities were measured with a calibrated silicon diode. The frequency-dependent light-modulated microwave and photocurrent responses were fitted using a nonlinear least squares program (Solartron Z-View). The flatband potential of the p-Si samples was determined from Mott Schottky plots to be +0.2 V vs Ag|AgCl prior to illumination.

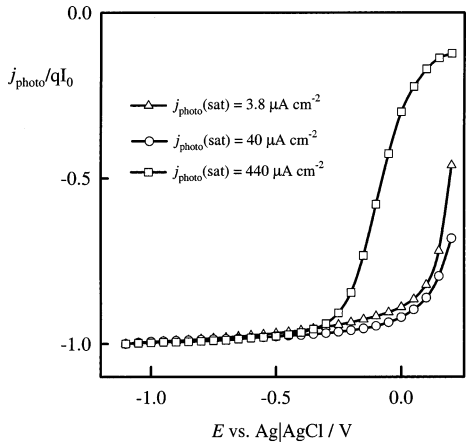

Figure 4. Normalized photocurrent voltage plots for p-Si in ammonium fluoride solution, pH 3.0 containing 0.33 mM $Ru(NH_3)_6^{3+}$. The values of the saturation photcourrent are shown. The displacement evident at the highest light intensity is attributed to exceeding the mass transport limited rate for reduction of $Ru((NH_3)_6^{3+}$, leading to accumulation of photogenerated electrons at the surface of p-Si.

Results and Discussion

"Steady State" Photocurrent and Microwave Responses. Figure 4 shows normalized photocurrent voltage plots for p-Si in a pH 3 fluoride solution containing 0.33 mM $Ru(NH_3)_6^{3+}$. At the two lowest light intensities, the photocurrent onset occurs close to the flatband potential (0.2 V vs Ag|AgCl). By contrast,

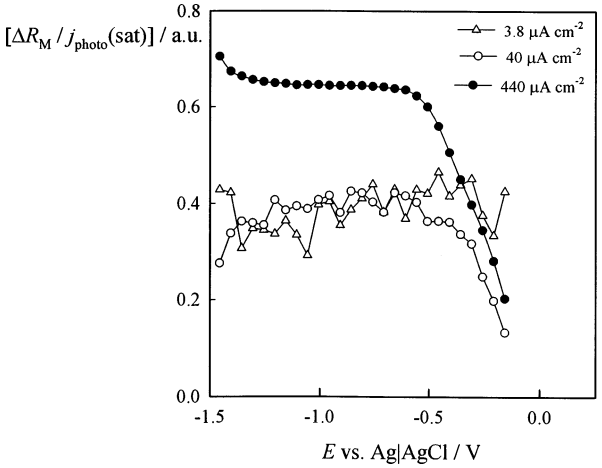

Figure 5. Normalized microwave reflectance plots obtained by dividing the microwave signal by the saturation photocurrent at each intensity (values shown). The higher response observed for the highest light intensity is interpreted as evidence for the accumulation of photogenerated electrons due to the onset of mass transport limitation in the reduction of $Ru(NH_3)_6^{3+}$ (concentration 0.33 mM).

at the highest light intensity, the photocurrent onset is shifted to more negative potentials. This indicates that the photocurrent in this case is larger than the limiting current for the mass transport controlled reduction of $Ru(NH_3)_6^{3+}$, so that hydrogen evolution occurs giving rise to surface charging.[5]

The corresponding normalized plots of the photoinduced microwave response are shown in Figure 5. It can be seen that the normalized microwave response is independent of light intensity at the lowest two illumination levels, but increases significantly at the highest light intensity. This is consistent with exceeding the mass transport controlled limiting current for Ru(III) reduction in the flow cell configuration, so that hydrogen evolution also occurs. To avoid mass transport limitations, LMMR and IMPS measurements were carried out at low light intensities, where the photocurrent in the plateau region was 3.6−3.9 μA cm^{-2}.

Comparison of the normalized magnitude of the measured microwave response for the two lowest light intensities with values predicted by numerical simulation as a function of k_{tr} (cf. Figure 2) suggests that $k_{tr} \approx 10^{-3}$ cm s^{-1}, not ≈ 1 cm s^{-1} as estimated for an outer sphere electron transfer process. In other words, the microwave response is much larger than expected, which indicates that electron transfer to redox species in solution is slow. (Note that Figure 1 shows the results of a calculation for $I_0 = 10^{14}$ cm^2 s^{-1}. The simulations showed that the microwave response should be a linear function of light intensity, so that normalization is straightforward.)

LMMR and IMPS. Figures 6 and 7 contrast the LMMR and IMPS plots obtained using a solution containing 0.33 mM Ru(III). It can be seen that the diameters of the LMMR plots become larger as the electrode potential is made more negative, increasing the band bending in the p-Si. On the other hand, the IMPS semicircles become smaller in diameter as the band bending is increased, until only a point on the real axis is observed in the limiting photocurrent region. It is noted here that the low-frequency data for the IMPS plots converge on the real axis, whereas in the case of the LMMR plots, the low-frequency response (not shown in Figure 7) tends to broaden along the real axis, suggesting an additional slow component.

The semicircular complex plane LMMR plots were fitted to obtain values of the low-frequency intercept and values of ω_{min}. These were used to obtain k_1 and k_{rec} as a function of potential.

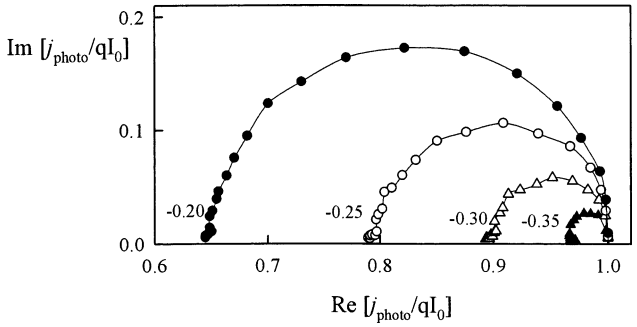

Figure 6. Normalized IMPS response plots at the potentials shown. The electrolyte contained 0.33 mM $Ru(NH_3)_6^{3+}$. Saturation photocurrent 3.6−3.9 μA cm^{-2}. The intercepts and ω_{min} values were used to obtain k_1 and k_{rec} as a function of potential.

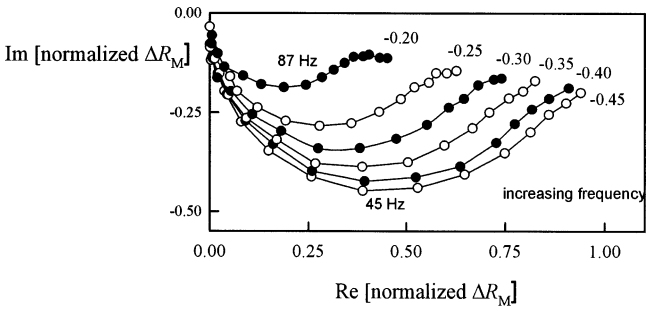

Figure 7. Normalized LMMR response plots at the potentials shown. The electrolyte contained 0.33 mM $Ru(NH_3)_6^{3+}$. Saturation photocurrent 3.6−3.9 μA cm^{-2}. The intercepts and ω_{min} values were used to obtain k_1 and k_{rec} as a function of potential (see Figure 8).

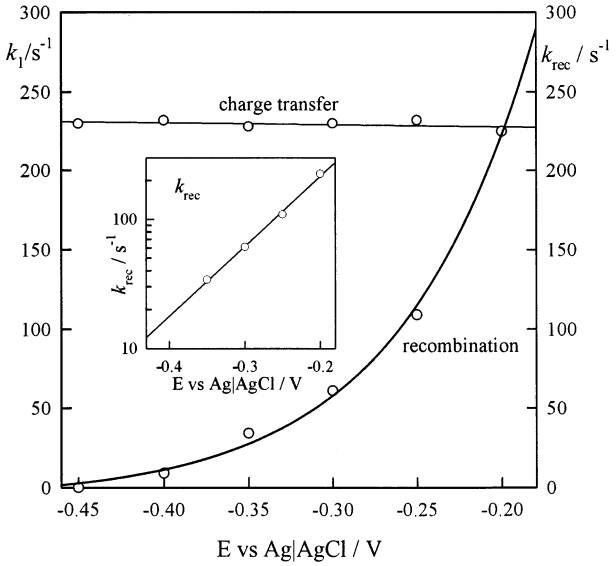

Figure 8. Potential dependence of k_1 and k_{rec} derived from the LMMR data shown in Figure 8. The inset shows the potential dependence of k_{rec} in a double logarithmic representation. Note that the rate constant for interfacial charge transfer is independent of potential over the entire range, whereas k_{rec} varies due to the change in hole density with potential.

Figure 8 shows the result. Over the range of potential investigated, k_1 was found to be remarkably constant (230 ± 5 s^{-1}), whereas k_{rec} varied exponentially with potential with a slope of (180 mV)$^{-1}$, as shown in the inset to Figure 7. Because surface recombination in p-Si is first order in the concentration of holes, one would expect a slope of (59 mV)$^{-1}$ for k_{rec} if the semiconductor|electrolyte junction behaved ideally and recombination occurred at the surface. The fact that the experimental slope is approximately 150 mV per decade could indicate that

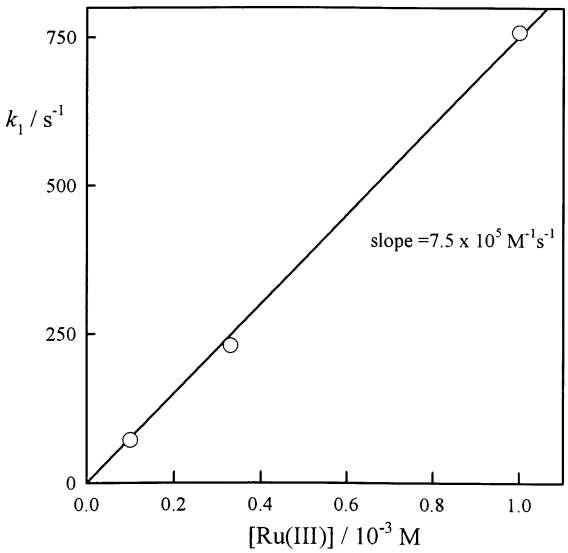

Figure 9. Concentration dependence of the phenomenological rate constant for electron transfer. The slope of the plot allows calculation of k_1 and k_2 (see text). The result confirms that the rate constants are much lower than predicted for an outer sphere electron transfer process.

the potential drop in the Helmholtz layer varies as a consequence of charging surface states.

The values of k_1 and k_{rec} obtained from the IMPS plots for a more restricted range of potential were similar to those obtained from the LMMR data, but as Figure 7 shows, the contraction of the IMPS plots with increasing band bending limited the range of potential over which an analysis could be performed. LMMR, by contrast, provides values of k_1 even when in the photocurrent saturation region, where recombination is negligible.

LMMR and IMPS measurements were repeated using different concentrations of $Ru(NH_3)_6^{3+}$ to check that the rate constant k_1 was first order in the concentration of redox species As Figure 9 shows, k_1 varies linearly with concentration as expected. The slope of the plot is 7.5×10^5 M^{-1} s^{-1}. Using eq 1 with $\delta \approx 10^{-7}$cm, we obtain $k_2 \approx 10^{-22}$ cm^4 s^{-1}, which is *4 orders of magnitude* lower than the value estimated for the outer sphere electron transfer process using eqs 2 and 3.

The very low value of k_2 suggests that capture of electrons at the surface of the illuminated p-Si involves a slow step. Our previous microwave reflectivity study of hydrogen evolution at p-Si in acidic fluoride media established that the electron transfer process was unusually slow.[5] Furthermore, there is a considerable body of evidence for hydrogen incorporation into silicon electrodes.[17−21] We have therefore proposed that conduction band electrons may be captured by protons to form subsurface protons as the first step of the hydrogen evolution process.[5] $Ru(NH_3)_6^{3+}$ could then scavenge hydrogen atoms that reach the surface. Navon and Meyerstein[22] have studied the reduction of $Ru(NH_3)_6^{3+}$ and $Co(NH_3)_6^{3+}$ by hydrogen atoms introduced from the gas phase. These authors reported identical values for the second-order rate constants (1.8×10^6 M^{-1} s^{-1}) for both complexes, suggesting that the rate constants are not determined by the reorganization energies. Instead, these authors proposed that an inner sphere mechanism is involved such as hydrogen abstraction or hydrogen insertion into the inner coordination sphere. It is not clear whether these mechanisms may be responsible for the slow reduction of $Ru(NH_3)_6^{3+}$ on p-Si. Another possibility is that the rate-determining step is the capture of electrons by protons or electron tunneling from near surface states. This process may be responsible for the additional slow component of the LMMR response noted earlier. The process is described by the sequence

$$H_3O^+ + e_{cb}^- \rightleftarrows H_{surf} + H_2O \quad (8a)$$

$$H_{surf} \rightleftarrows H_{Si} \quad (8b)$$

$$H_{Si} \rightleftarrows H_{Si}^+ + e_{cb}^- \quad (8c)$$

$$H_{surf} + Ru(NH_3)_6^{3+} + H_2O \rightarrow H_3O^+ + Ru(NH_3)_6^{2+} \quad (8d)$$

In this scheme, hydrogen penetrates into the near surface of the p-Si, where it can act as a "near surface state". (Such near surface states interact more strongly with the semiconductor than with the solution because interfacial electron transfer is limited by tunneling.) Atom exchange with the surface by eq 8b and electron exchange with the conduction band are represented by eq 8c. Alternatively, protons may penetrate into the Si lattice so that electrons are captured before they reach the surface. In this case, electron capture by protons would be favored as the first step and the loci for the competing electron transfer reactions would be different. Similar behavior has been observed in the case of p-GaP,[23] where the term "near surface state" has been used to underline the importance of the spatial distribution of electron acceptors. Such near surface states should be very effective in intercepting electrons before they can be transferred to redox species in solution. The subsequent transfer of the trapped electron to redox species could be slow due to tunneling effects or to diffusion of hydrogen atoms.

Conclusions

The present study has shown how light modulated microwave reflectivity measurements can be used to investigate electron transfer at illuminated semiconductor electrodes. Comparison of the measured rate constants for electron transfer with theoretical predictions indicates that the mechanism of reduction of $Ru(NH_3)_6^{3+}$ cannot involve direct electron transfer from the conduction band. Instead it appears that electron transfer is mediated by hydrogen surface states.

Acknowledgment. This work was supported by the UK Engineering and Physical Science Research Council (EPSRC). We thank Alison Walker, Michael Cass, and Steve Pennock for assistance with the modeling of the microwave response as well as Noel Duffy, Mike Bailes, and David Hatten for assistance with the experimental system.

References and Notes

(1) Peter, L. M. *Chem. Rev.* **1990**, *90*, 753.
(2) Peter, L. M.; Vanmaekelbergh, D. Time and frequency resolved studies of photoelectrochemical kinetics. In *Advances in Electrochemical Science and Engineering*; Alkire, R., Kolb, D. M., Eds.; Weinheim, 1999; Vol. 6, p 77.
(3) Schlichthörl, G.; Ponomarev, E. A.; Peter, L. M. *J. Electrochem. Soc.* **1995**, *142*, 3062.
(4) Cass, M. J.; Duffy, N. W.; Peter, L. M.; Pennock, S. R.; Ushiroda, S.; Walker, A. B. *J. Phys. Chem. B* **2003**, *107*, 5857.
(5) Cass, M. J.; Duffy, N. W.; Peter, L. M.; Pennock, S. R.; Ushiroda, S.; Walker, A. B. *J. Phys. Chem. B* **2003**, *107*, 5864.
(6) Schlichthörl, G.; Tributsch, H. *Electrochim. Acta* **1992**, *37*, 919.
(7) Tributsch, H. Microwave (Photo)electrochemistry. In *Modern Aspects of Electrochemistry*; White, R. E., Ed.; Kluwer Academic/Plenum Publishers: New York, 1999; Vol. 33, p 435.
(8) Tributsch, H.; Schlichthörl, G.; Elstner, L. *Electrochim. Acta* **1993**, *38*, 141.
(9) Forbes, M. D. E.; Lewis, N. S. *J. Am. Chem. Soc.* **1990**, *112*, 3682.
(10) Peter, L. M.; Ponomarev, E. A.; Fermin, D. J. *J. Electroanal. Chem.* **1997**, *427*, 79.

(11) Morrison, S. R. *Electrochemistry of semiconductor and metal electrodes*; Plenum Press: New York, 1980.
(12) Smolenaers, P. J.; Beattie, J. K. *Inorg. Chem.* **1986**, *25*, 2259.
(13) Pomykal, K. E.; Lewis, N. S. *J. Phys. Chem. B* **1997**, *101*, 2476.
(14) Royea, W. J.; Fajardo, A. M.; Lewis, N. S. *J. Phys. Chem. B* **1998**, *102*, 3653.
(15) Royea, W. J.; Fajardo, A. M.; Lewis, N. S. *J. Phys. Chem. B* **1997**, *101*, 11152.
(16) Fajardo, A. M.; Lewis, N. S. *J. Phys. Chem. B* **1997**, *101*, 11136.
(17) Belaidi, A.; Chazalviel, J. N.; Ozanam, F.; Gorochov, O.; Chari, A.; Fotouhi, B.; Etman, M. *J. Electroanal. Chem.* **1998**, *444*, 55.
(18) Mandal, K. C.; Ozanam, F.; Chazalviel, J. N. *Appl. Phys. Lett.* **1990**, *57*, 2788.
(19) de Mierry, P.; Etcheberry, A.; Rizk, R.; Etchegoin, P.; Aucouturier, M. *J. Electrochem. Soc.* **1994**, *141*, 1539.
(20) de Mierry, P.; Etcheberry, A.; Aucouturier, M. *Physica B (Amsterdam)* **1991**, *170*, 124.
(21) de Mierry, P.; Etcheberry, A.; Aucouturier, M. *J. Appl. Phys.* **1991**, *69*, 1099.
(22) Navon, G.; Meyerstein, D. *J. Phys. Chem.* **1970**, *74*, 4067.
(23) Li, J.; Peat, R.; Peter, L. M. *J. Electroanal. Chem. Interfacial Electrochem.* **1984**, *165*, 41.